A Two-Dimensional Extension of the Mueller & Müller Timing Error Detector

Kevin M. Whelan * *Student Member, IEEE,* Félix Balado *Member, IEEE,* Guénolé C.M. Silvestre *Member, IEEE,* and Neil J. Hurley

Abstract

A timing error detector (TED) forms an integral part of feedback symbol timing recovery systems in digital communications. We present here a two-dimensional (2-D) extension of a TED originally developed by Mueller and Müller for multi-level pulse amplitude modulation (PAM) over one-dimensional (1-D) channels. Our detector extracts bidimensional timing information (i.e., bidimensional sampling information) from the output of a noisy channel with bidimensional transfer function and subject to sampling errors. Applications for such a scenario include synchronization in multi-level 2-D bar code systems and synchronization in spatial domain image data-hiding. To our knowledge, our proposal is the first one of its kind for this type of scenario. We provide accurate theoretical expressions of the performance of the proposed scheme, and we verify its applicability by studying a particular case with a minimal set of parameters. The 2-D TED thus obtained is used as the engine of a 2-D phase locked loop (PLL) for timing recovery in that scenario, in which we also show the performance gain obtained by the bidimensional approach with respect to the application of standard 1-D TED.

EDICS Category: IMD-MDSP, COM-ESTI

*Corresponding author. E-mail: kevin.whelan@ihl.ucd.ie; Phone: +353 1 716 2454; Fax: +353 1 269 7262

All the authors are with the School of Computer Science and Informatics at University College Dublin (National University of Ireland). Common address: University College Dublin, School of Computer Science and Informatics, Belfield Campus, Dublin 4, Ireland. E-mails: Félix Balado: fiz@ihl.ucd.ie; Guénolé C.M. Silvestre: guenole.silvestre@ihl.ucd.ie; Neil J. Hurley: neil.hurley@ucd.ie. Their phone and fax numbers are the same as for the corresponding author. This work was kindly supported by Enterprise Ireland under the research grant ATRP-2002/230 and by the European Commission through the IST Programme under Contract IST-2002-507609 SIMILAR.

A Two-Dimensional Extension of the Mueller & Müller Timing Error Detector

I. Introduction

A common approach to timing recovery in a digital communications system is to estimate the timing parameters from the received signal using a digital PLL. The main building block of a PLL is a TED, which computes the timing error signal required by the synchronization device. A number of TEDs have been developed for timing recovery on temporal channels with one-dimensional impulse response, in which the transfer function depends on a scalar variable (time). Nevertheless, in some relatively recent applications the channel intrinsically exhibits a two-dimensional impulse response, usually as a result of the spatial configuration of the communications problem tackled. Sampling errors (i.e., synchronization errors) in these channels are spatial rather than temporal. Then, we may talk in these cases of spatial sampling grid recovery instead of timing recovery, although in this work we will use the latter term in keeping with the usual synchronization terminology. In order to perform PLL-based timing recovery on two-dimensional settings a 2-D PLL —and then a 2-D TED— is required. To our knowledge, there are no previous works that address the problem of synchronization in bidimensional communication channels, which prompts us to propose one such scheme in this letter. Our proposal departs from the well-known TED developed by Mueller and Müller for timing recovery in multi-level PAM systems [1], which we denote by M&M TED. Although in part superseded by later, more advanced designs, this TED has recently received renewed interest through its applicability as a key building block in state-of-the-art iterative synchronization schemes [2]. Here we extend the 1-D M&M TED to work over a 2-D channel impulse response. The applications for a 2-D M&M TED include synchronization in multi-level 2-D bar code systems [3], [4], and also synchronization of spatial domain image data-hiding along the same guidelines described in [5] for a 1-D setting.

In this letter, we present initially an extension of the procedures outlined in [1] to an equivalent bidimensional setting. The results of this extension are then applied to a specific scenario, in order to develop a concrete realization of the 2-D M&M TED. We finally show the performance improvement offered by this strategy when compared to the separate use of 1-D M&M TEDs in a 2-D scenario.

a) Notation and Setting Assumptions: Upper case bold types denote matrices e.g., $\mathbf{X}$, with elements denoted $x_{i,j}$. Lower case bold types denote vectors, e.g., $\mathbf{x}$, which are arranged columnwise. The zero vector is denoted by $\mathbf{0}$ and the all-ones vector by $\mathbf{1}$. $\|\mathbf{x}\|$ denotes the Euclidean norm of $\mathbf{x}$, and $\mathrm{tr}(\mathbf{X})$ the trace of $\mathbf{X}$. For notational simplicity we will make use of *vector* indices, i.e., $\mathbf{i} \triangleq (i_1, i_2)^T \in \mathbb{Z}^2$, so that a matrix element x_{i_1,i_2} may equivalently be denoted $x_{\mathbf{i}}$. The context indicates in most cases if a vector symbol is a vector index, and therefore we will only make this point explicit when there may exist ambiguity. In the setting considered we wish to perform PLL-based synchronization on a two-dimensional M-ary PAM system in which an $N \times N$ matrix $\mathbf{A}$ of independent and identically distributed (i.i.d.) data symbols is transmitted through a bidimensional channel with desynchronization. An individual symbol is for instance $a_{\mathbf{i}} \in \mathcal{A} \subset \mathbb{R}$, with $\mathcal{A}$ of cardinality $|\mathcal{A}| = M$, and the k-th moment of the symbols is denoted $\mathrm{E}[a^k]$. The channel is modelled by an overall 2-D impulse response $h(\mathbf{t})$, where $\mathbf{t} = (t_1, t_2)^T \in \mathbb{R}^2$, and additive i.i.d. Gaussian noise. $h(\mathbf{t})$ accounts for any transmission pulse shaping and/or channel transfer function. The continuous output of this channel can be described by $z(\mathbf{t}) = \sum_{\mathbf{i}} a_{\mathbf{i}} h(\mathbf{t} - \mathbf{i}T - \boldsymbol{\tau}) + n(\mathbf{t})$, where $n(\mathbf{t})$ is zero-mean white Gaussian noise with variance σ_n^2, T is the spatial sampling period, and $\boldsymbol{\tau} = (\tau_1, \tau_2)^T \in \mathbb{R}^2$ represents an unknown constant sampling offset introduced by the channel. The signal $z(\mathbf{t})$ is sampled by the receiver at points $\{\mathbf{j}T + \hat{\boldsymbol{\tau}}\}$, where $\mathbf{j} \in \mathbb{Z}^2$ and $\hat{\boldsymbol{\tau}}$ is an estimate of $\boldsymbol{\tau}$ produced by the synchronization system in the receiver. The sampled received signal is then given by the $N \times N$ matrix $\mathbf{Z}$ with elements

$$z_{\mathbf{j}} = \sum_{\mathbf{i}} a_{\mathbf{i}}\, h_{\mathbf{j}-\mathbf{i}} + n_{\mathbf{j}}, \tag{1}$$

with $z_{\mathbf{j}} \triangleq z(\mathbf{j}T + \boldsymbol{\epsilon})$, $h_{\mathbf{j}} \triangleq h\big(\mathbf{j}T + \boldsymbol{\epsilon}\big)$, $\boldsymbol{\epsilon} \triangleq \hat{\boldsymbol{\tau}} - \boldsymbol{\tau}$ and $n_{\mathbf{j}}$ i.i.d. noise samples with $n_{\mathbf{j}} \sim \mathcal{N}(0, \sigma_n^2)$. The task of the TED is to produce an estimate of the timing error $\boldsymbol{\epsilon} = (\epsilon_1, \epsilon_2)^T$ from the samples of the received signal. This error signal $\boldsymbol{\epsilon}$ is used to adjust the PLL estimates of the correct sampling points. The received signal is then resampled using this adjusted information.

II. Two-dimensional Timing Error Detector

In the setting considered, the receiver has to estimate a vectorial timing error. We present next a two-dimensional extension of the procedure outlined in [1] for estimating a scalar timing error. As in that work, the first step is to build an ideal timing function $\tilde{\mathbf{f}}(\cdot) : \mathbb{R}^2 \to \mathbb{R}^2$ using a linear combination of samples of $h(\mathbf{t})$ offset by the actual sampling error $\boldsymbol{\epsilon}$, i.e., $h_{\mathbf{i}} = h(\mathbf{i}T + \boldsymbol{\epsilon})$. For this function of the timing error $\tilde{\mathbf{f}}(\boldsymbol{\epsilon}) = \boldsymbol{\epsilon}$ holds ideally. Following the type A class of functions described in [1], and for certain relevant types of $h(\mathbf{t})$ that will be described next, we can build and approximation $\mathbf{f}(\cdot)$ to the required function $\tilde{\mathbf{f}}(\cdot)$ with components

$$f_1(\boldsymbol{\epsilon}) = \frac{1}{2}(h_{-1,0} - h_{1,0}) \approx \epsilon_1, \qquad f_2(\boldsymbol{\epsilon}) = \frac{1}{2}(h_{0,-1} - h_{0,1}) \approx \epsilon_2. \tag{2}$$

As an example, Figure 1 shows $f_1(\boldsymbol{\epsilon})$ for the case where $h(\cdot)$ is a separable 2-D filter $h(\mathbf{t}) = \bar{h}(t_1) \cdot \bar{h}(t_2)$, and $\bar{h}(t) = \mathrm{sinc}(t/T)$. We can see that $f_1(\boldsymbol{\epsilon})$ approximates reasonably well the ideal function in an environment of $\boldsymbol{\epsilon} = \mathbf{0}$ given roughly by $|\epsilon_1|, |\epsilon_2| < 0.2$. Due to the symmetry of the $h(\mathbf{t})$ chosen, $f_2(\boldsymbol{\epsilon})$ exhibits the same behavior. Note that separability of the filter is not a requirement on $h(\cdot)$. For instance, the non-separable version of the above filter, i.e., $h(\mathbf{t}) = \mathrm{sinc}\left(\|\mathbf{t}\|/T\right)$, yields almost identical behavior of the timing functions. Different $h(\mathbf{t})$ will obviously change the shape of the functions (2). However any impulse response approximating $\mathrm{sinc}(\|\mathbf{t}\|/T)$ will yield similar timing functions. For example, in an image data hiding application it is reasonable to assume that $h(\mathbf{t})$ will be a close approximation to the ideal interpolation filter $\mathrm{sinc}(\|\mathbf{t}\|/T)$ in order to minimize the perceptual degradation of the image. Therefore we can expect similar timing functions to those in Figure 1.

Following [1], as the actual $h_{\mathbf{i}}$ in (2) are not known, it is necessary now to estimate $\mathbf{f}(\boldsymbol{\epsilon})$ from a group of past samples of $z(\mathbf{t})$. In the one-dimensional temporal case the notion of past is natural and obvious; nevertheless, in our spatial context we need to establish first a definition for what "past" means.

A. Path & Past in Two Dimensions

We define a *path* scanning all the elements of an $N \times N$ matrix $\mathbf{Z}$ as an ordered set $(\mathcal{P}, \leq)$ of N^2 distinct vector indices with spatial continuity constraints. Defining $\mathcal{W} \triangleq \{1, \cdots, N\}$, a path is then given by $\mathcal{P} \triangleq \{\mathbf{p}(1), \mathbf{p}(2) \cdots, \mathbf{p}(N^2) : \mathbf{p}(k) \in \mathcal{W}^2$ for all $k = 1, \cdots, N^2\}$, such that $\cup_{k=1}^{N^2} \mathbf{p}(k) = \mathcal{W}^2$ and $\|\mathbf{p}(k) - \mathbf{p}(k+1)\|^2 \leq 2$ for all $k = 1, \cdots, N^2 - 1$. We define the order relationship on $\mathcal{P}$ as $\mathbf{p}(n) \leq \mathbf{p}(m)$ iff $n \leq m$, for any two valid indices n, m. $\mathcal{P}$ provides a sequential way to index all the elements of $\mathbf{Z}$, which is necessary because of the sequentiality of estimation and decoding. This type of path includes the well-known JPEG compression zig-zag scanning, but excludes the typical left-right line scanning. The latter is also possible if the spatial constraint is not applied to elements indexing the boundary of the matrix $\mathbf{Z}$, which is the criterion we adopt in the following.

In keeping with the notion of past in a one-dimensional setting, we may view the path $\mathcal{P}$ as a "temporal" sequence. Then, at "time" k the causal part of $\mathcal{P}$, i.e., its past, is defined as the ordered subset $\mathcal{P}_k \triangleq \{\mathbf{p} \in \mathcal{P} :\ \mathbf{p} \leq \mathbf{p}(k)\}$. Notice that some elements of $\mathcal{P}_k$ may be closer spatially than "temporally", depending on the path chosen. Elements which are too far away spatially will not be useful for estimation purposes, and then it seems sensible to observe the past only in a spatial neighborhood, for instance:

$$\mathcal{P}_k^{(d)} \triangleq \{\mathbf{p} \in \mathcal{P}_k :\ \|\mathbf{p}(k) - \mathbf{p}\|^2 \leq d\}, \tag{3}$$

with $d \geq 1$. The size of this ordered subset is $m \triangleq |\mathcal{P}^{(d)}|$, which we assume independent of k neglecting border effects. Past spatial vicinities other than (3) do not change substantially our exposition next.

B. Estimating the Timing Functions from the Received Signal

We follow next the procedure in [1] for estimating a timing function in a one-dimensional setting, adapting it to our two-dimensional set-up. Choosing first a path $\mathcal{P}$, we have to build an estimate of $\mathbf{f}(\boldsymbol{\epsilon}) = \big(f_1(\boldsymbol{\epsilon}), f_2(\boldsymbol{\epsilon})\big)^T$ at time k as a linear combination of the past elements of $\mathbf{Z}$. As $\mathbf{f}(\boldsymbol{\epsilon}) \approx \boldsymbol{\epsilon}$ we denote the estimate of $\mathbf{f}(\boldsymbol{\epsilon})$ at time k as $\hat{\boldsymbol{\epsilon}}_k = (\hat{\epsilon}_{1,k}, \hat{\epsilon}_{2,k})^T$. This estimate should satisfy $\mathrm{E}[\hat{\boldsymbol{\epsilon}}_k] = \mathbf{f}(\boldsymbol{\epsilon})$ and, according to the previous exposition, is obtained as

$$\hat{\boldsymbol{\epsilon}}_k = \mathbf{G}_k \, \mathbf{z}_k,$$

with $\mathbf{z}_k$ defined as the $m \times 1$ vector formed by the past m samples of $\mathbf{Z}$ indexed by $\mathcal{P}_k^{(d)}$, i.e.,

$$\mathbf{z}_k^T \triangleq \big(z_{\mathbf{p}(k-m+1)}, \cdots, z_{\mathbf{p}(k)}\big),$$

and $\mathbf{G}_k \triangleq (\mathbf{g}_{1,k} \,|\, \mathbf{g}_{2,k})^T$ a $2 \times m$ matrix formed by the weighting vectors $\mathbf{g}_{1,k}$ and $\mathbf{g}_{2,k}$, to be obtained according to the problem constraints. Now,

$$\mathrm{E}[\hat{\boldsymbol{\epsilon}}_k] = \mathrm{E}[\mathbf{G}_k \, \mathbf{z}_k] = \mathrm{E}[\mathrm{E}[\mathbf{G}_k \, \mathbf{z}_k | \mathbf{a}_k]] = \mathrm{E}[\mathbf{G}_k \, \mathbf{v}_k], \tag{4}$$

with $\mathbf{a}_k$ defined as $\mathbf{z}_k$ using the past m symbols, and $\mathbf{v}_k \triangleq \mathrm{E}[\mathbf{z}_k | \mathbf{a}_k]$. The l-th element of $\mathbf{v}_k$ is

$$[\mathbf{v}_k]_l = \mathrm{E}[z_{\mathbf{p}(k-m+l)} | \mathbf{a}_k] = \sum_{\mathbf{r} \in \mathcal{P}_k^{(d)}} a_{\mathbf{r}} \, h_{\mathbf{p}(k-m+l)-\mathbf{r}}. \tag{5}$$

Notice that the computation of each of the m elements of $\mathbf{v}_k$ involves m samples of the impulse response. The sample $h_{\mathbf{0}}$ is common to all elements, resulting in a maximum of $m^2 - m$ samples of $h(\cdot)$ involved in computing $\mathbf{v}_k$. Depending on how $\mathcal{P}_k^{(d)}$ is defined, certain samples of $h(\cdot)$ may be involved in more than one $[\mathbf{v}_k]_l$. If we define next a $c \times 1$ vector $\mathbf{h}$, $c \leq m^2 - m$, containing the arbitrarily arranged *unique* samples of $h(\cdot)$ used to compute $\mathbf{v}_k$, we can write

$$\mathbf{v}_k = \mathbf{A}_k^T \mathbf{h}, \tag{6}$$

with $\mathbf{A}_k$ a $c \times m$ matrix, each column of which contains the m elements of $\mathbf{a}_k$ arranged to satisfy (5) for a given $\mathbf{h}$ and with zeros filled in elsewhere. Using (4) and (6) we may write $\mathrm{E}[\hat{\epsilon}_{l,k}] = \mathbf{h}^T \mathrm{E}[\mathbf{A}_k \mathbf{g}_{l,k}]$, for $l = 1, 2$. Notice that the timing functions (2) may be written as

$$f_l(\boldsymbol{\epsilon}) = \mathbf{h}^T \mathbf{u}_l, \qquad l = 1, 2 \,, \tag{7}$$

with $\mathbf{u}_l$ a $c \times 1$ vector of weights which can be deduced from (2) and $\mathbf{h}$. Our objective then is to choose $\mathbf{g}_{l,k}$ such that $\mathrm{E}[\mathbf{A}_k \mathbf{g}_{l,k}] = \mathbf{u}_l$ for $l = 1, 2$. It is easy to verify that all these definitions boil down to the known ones in [1] for the one-dimensional case, in which case $\mathcal{P}_k$ becomes the causal past of the one-dimensional signal.

b) Variance of the Estimators: The procedure outlined in [1] to calculate the variance of their one-dimensional timing function estimator can be also restated for the two-dimensional case, and then used to compute the variance of $\hat{\epsilon}_{l,k}$, for $l = 1, 2$. We begin with the evaluation of the second moment of $\mathrm{E}[\hat{\epsilon}^2_{l,k}] = \mathrm{E}[\mathbf{g}^T_{l,k}\mathbf{z}_k\mathbf{z}^T_k\mathbf{g}_{l,k}] = \mathrm{E}[\mathbf{g}^T_{l,k}\mathrm{E}[\mathbf{z}_k\mathbf{z}^T_k|\mathbf{a}_k]\mathbf{g}_{l,k}]$. The elements of the $m \times m$ matrix $\mathbf{M}_k \triangleq \mathrm{E}[\mathbf{z}_k\mathbf{z}^T_k|\mathbf{a}_k]$ are given by

$$m_{i,j} = \mathrm{E}[[\mathbf{z}_k]_i[\mathbf{z}_k]_j|\mathbf{a}_k] = \sum_{\mathbf{r}}\sum_{\mathbf{s}} \mathrm{E}[a_{\mathbf{r}}a_{\mathbf{s}}|\mathbf{a}_k]\, h_{\mathbf{p}(k-m+i)-\mathbf{r}}\, h_{\mathbf{p}(k-m+j)-\mathbf{s}}. \tag{8}$$

As the data symbols are assumed to be i.i.d. (8) may be rewritten (see [1]) as

$$m_{i,j} = \sum_{\mathbf{r}\in\mathcal{P}^{(d)}_k}\sum_{\mathbf{s}\in\mathcal{P}^{(d)}_k} a_{\mathbf{r}}a_{\mathbf{s}}h_{\mathbf{p}(k-m+i)-\mathbf{r}}\, h_{\mathbf{p}(k-m+j)-\mathbf{s}} + \mathrm{E}[a^2]\sum_{\mathbf{r}\notin\mathcal{P}^{(d)}_k} h_{\mathbf{p}(k-m+i)-\mathbf{r}}\, h_{\mathbf{p}(k-m+j)-\mathbf{r}}. \tag{9}$$

Observing (5), the matrix $\mathbf{M}_k$ may be rewritten as $\mathbf{M}_k = \mathbf{v}_k\mathbf{v}^T_k + \mathbf{Q}$, where the elements of $\mathbf{Q}$ are given by the second term in (9). The second moment of $\hat{\epsilon}_{l,k}$ may now be written as

$$\mathrm{E}[\hat{\epsilon}^2_{l,k}] = \mathrm{E}[\mathbf{g}^T_{l,k}(\mathbf{v}_k\mathbf{v}^T_k + \mathbf{Q})\mathbf{g}_{l,k}] = \mathrm{E}[(\mathbf{g}^T_{l,k}\mathbf{v}_k)^2 + \mathbf{g}^T_{l,k}\mathbf{Q}\mathbf{g}_{l,k}],$$

and then, using the expectation, the variance is just

$$\mathrm{Var}[\hat{\epsilon}_{l,k}] = \mathrm{E}[(\mathbf{g}^T_{l,k}\mathbf{v}_k)^2] + \mathrm{E}[\mathbf{g}^T_{l,k}\mathbf{Q}\mathbf{g}_{l,k}] - \mathrm{E}^2[\mathbf{g}^T_{l,k}\mathbf{v}_k]. \tag{10}$$

Following [1], as the noise terms $n_{\mathbf{j}}$ in (1) are zero mean i.i.d., the effect of noise addition on the variance can be included in the above analysis by replacing $\mathbf{Q}$ with $\mathbf{Q} + \sigma^2_n\mathbf{I}$, with $\mathbf{I}$ the $m \times m$ identity matrix.

III. Derivation of the Weights for Specific Path & Past

The objective now is to choose the weighting vectors $\mathbf{g}_{l,k}$ such that the constraint $\mathrm{E}[\mathbf{A}_k\mathbf{g}_{l,k}] = \mathbf{u}_l$ for $l = 1, 2$ is met. As discussed in [1], the optimum $\mathbf{g}^*_{l,k}$ that minimizes the variance (10) depends on channel parameters unknown to the receiver, but it is possible to pursue a suboptimal approach solving the weights as the following channel-independent linear problem:

$$\mathbf{A}_k\mathbf{g}_{l,k} = \mathbf{u}_l + \mathbf{d}_{l,k}, \qquad \text{for } l = 1, 2, \tag{11}$$

with $\mathbf{d}_{l,k}$ a zero-mean random vector chosen to meet the problem constraints. $\mathbf{u}_l$ is given by (7) and will determine the selection of $\mathbf{g}_{l,k}$ and $\mathbf{d}_{l,k}$. It is important that $\mathrm{tr}(\mathrm{Var}[\mathbf{d}_{l,k}\mathbf{d}^T_{l,k}])$ should be kept small, as

$$\mathrm{Var}[\hat{\epsilon}_{l,k}] = \mathrm{E}[(\mathbf{h}^T\mathbf{d}_{l,k})^2 + \mathbf{g}^T_{l,k}\mathbf{Q}\mathbf{g}_{l,k}]. \tag{12}$$

The component of $\mathbf{d}_{l,k}$ associated with $h_{\mathbf{0}}$ must be zero to ensure the variance is independent of $h_{\mathbf{0}}$ when $z(\mathbf{t})$ is sampled at the correct points.

We discuss next how to solve (11) for a specific path and past. Taking $\mathcal{P}$ as the left-to-right scan and the past $\mathcal{P}_k^{(2)}$ we have that $m = 5$. If the current vector index $\mathbf{p}(k)$ is given by $(i,j)^T$, then $\mathcal{P}_k^{(2)} = \{(i-1,j-1)^T, (i-1,j)^T, (i-1,j+1)^T, (i,j-1)^T, (i,j)^T\}$. In order to facilitate an algebraic solution we modify $\mathcal{P}_k^{(2)}$ by removing $(i-1,j+1)^T$; the effect of this operation will be discussed in Sect. IV. Then, $m = 4$ and $\mathbf{z}_k^T = (z_{i-1,j-1}, z_{i-1,j}, z_{i,j-1}, z_{i,j})$. Now, for this $\mathcal{P}_k^{(2)}$ we take the unique samples of $h(\cdot)$ involved in computing (5) in the following arbitrary arrangement

$$\mathbf{h}^T = (h_{-1,-1}\ ,\ h_{-1,0}\ ,\ h_{-1,1}\ ,\ h_{0,-1}\ ,\ h_{0,0}\ ,\ h_{0,1}\ ,\ h_{1,-1}\ ,\ h_{1,0}\ ,\ h_{1,1}). \tag{13}$$

For this $\mathbf{h}$, the matrix $\mathbf{A}_k$ in (6) takes the following form

$$\mathbf{A}_k^T = \begin{pmatrix} a_{i,j} & a_{i,j-1} & 0 & a_{i-1,j} & a_{i-1,j-1} & 0 & 0 & 0 & 0 \\ 0 & a_{i,j} & a_{i,j-1} & 0 & a_{i-1,j} & a_{i-1,j-1} & 0 & 0 & 0 \\ 0 & 0 & 0 & a_{i,j} & a_{i,j-1} & 0 & a_{i-1,j} & a_{i-1,j-1} & 0 \\ 0 & 0 & 0 & 0 & a_{i,j} & a_{i,j-1} & 0 & a_{i-1,j} & a_{i-1,j-1} \end{pmatrix}. \tag{14}$$

Now, using (13) and (14) we solve (11) for $\mathbf{u}_l$, $l = 1,2$ to build an estimator of $f_l(\boldsymbol{\epsilon})$.

A. Estimating $f_1(\boldsymbol{\epsilon})$ and $f_2(\boldsymbol{\epsilon})$

Using the first function in (2), (7) and (13), we have that the vector $\mathbf{u}_1$ has to take the form $\mathbf{u}_1^T = (0, \frac{1}{2}, 0, 0, 0, 0, 0, -\frac{1}{2}, 0)$. Then, a solution to (11) is $\mathbf{g}_{1,k}^T = (a_{i,j-1}, a_{i,j}, -a_{i-1,j-1}, -a_{i-1,j})/4\mathrm{E}[a^2]$, with

$$\mathbf{d}_{1,k} = \frac{1}{4\mathrm{E}[a^2]} \begin{pmatrix} a_{i,j-1} \cdot a_{i,j} \\ -2\mathrm{E}[a^2] + a_{i,j-1}^2 + a_{i,j}^2 \\ a_{i,j-1} \cdot a_{i,j} \\ a_{i-1,j} \cdot a_{i,j-1} - a_{i-1,j-1} \cdot a_{i,j} \\ 0 \\ -a_{i-1,j} \cdot a_{i,j-1} + a_{i-1,j-1} \cdot a_{i,j} \\ -a_{i-1,j-1} \cdot a_{i-1,j} \\ 2\mathrm{E}[a^2] - a_{i-1,j-1}^2 - a_{i-1,j}^2 \\ -a_{i-1,j-1} \cdot a_{i-1,j} \end{pmatrix}, \tag{15}$$

yielding the timing error estimate

$$\hat{\epsilon}_{1,k} = (\,-z_{i,j}a_{i-1,j} - z_{i,j-1}a_{i-1,j-1} + z_{i-1,j}a_{i,j} + z_{i-1,j-1}a_{i,j-1})/4\mathrm{E}[a^2]. \tag{16}$$

Notice that, as required, $\mathrm{E}[\hat{\epsilon}_{1,k}] = (h_{-1,0} - h_{1,0})/2$ (cf. first equation in (2)) and $\mathrm{E}[\mathbf{d}_{1,k}] = \mathbf{0}$. Using now the second function in (2), (7) and (13) we have that $\mathbf{u}_2^T = (0,0,0,\frac{1}{2},0,-\frac{1}{2},0,0,0)$. As before, one solution to (11) is $\mathbf{g}_{2,k}^T = (a_{i-1,j}, -a_{i-1,j-1}, a_{i,j}, -a_{i,j-1})/4\mathrm{E}[a^2]$. $\mathbf{d}_{2,k}$ follows similarly to (15) from (11), and using the vectors $\mathbf{u}_2$ and $\mathbf{g}_{2,k}$; we omit the expression here for brevity. The resulting timing error estimate is given by

$$\hat{\epsilon}_{2,k} = (-z_{i,j}a_{i,j-1} + z_{i,j-1}a_{i,j} - z_{i-1,j}a_{i-1,j-1} + z_{i-1,j-1}a_{i-1,j})/4\mathrm{E}[a^2]. \tag{17}$$

Again, it can be shown that $\mathrm{E}[\hat{\epsilon}_{2,k}] = (h_{0,-1} - h_{0,1})/2$ and $\mathrm{E}[\mathbf{d}_{2,k}] = \mathbf{0}$.

The timing error estimators (16) and (17) are completely parallel to the one obtained by Mueller & Müller in one dimension, but of course, more cross-products show up in these estimates due to the two-dimensional nature of the set-up. The appearance of the data symbols $a_{i,j}$ in the estimators leads to two possible modes of operation. In data-aided (DA) mode, the symbols are known *a priori* to the receiver. Alternatively in decision-directed (DD) mode, estimates $\hat{a}_{i,j}$ are first made on the transmitted symbols and used in place of their actual values in (16) and (17).

Using (12) it is tedious but straightforward to compute the variance of (16) and (17). For $\hat{\epsilon}_1$

$$\mathrm{Var}[\hat{\epsilon}_{1,k}] = \frac{1}{4}\sum_{\mathbf{p}\neq\mathbf{0}} h_{\mathbf{p}}^2 - \left(2 - \frac{\mathrm{E}[a^4]}{\mathrm{E}^2[a^2]}\right)\frac{h_{-1,0}^2 + h_{1,0}^2}{8} + \frac{1}{8}(h_{-1,-1}h_{-1,1} + h_{1,-1}h_{1,1} - 2h_{0,1}h_{0,-1}) + \frac{\sigma_n^2}{4\mathrm{E}[a^2]}. \tag{18}$$

A similar expression can be derived for $\mathrm{Var}[\hat{\epsilon}_{2,k}]$, but it is omitted here due to space constraints.

IV. Experimental Results and Comparison with 1-D M&M TED

We examine here the performance of the proposed 2-D TED when operating on the output of a 4-PAM system over a channel with overall impulse response given by the separable filter in Sect. II. Figure 1 shows $\mathrm{E}[\hat{\epsilon}_{1,k}]$ as a function of $\boldsymbol{\epsilon}$ with the TED operating in DA mode and $\mathrm{SNR} = \mathrm{E}[a^2]/\sigma_n^2$. If the TED is operated in DD mode the range of $\boldsymbol{\epsilon}$ for which $\mathrm{E}[\hat{\epsilon}_{1,k}] = f_1(\boldsymbol{\epsilon})$ decreases. This is due to the reliability decrease of the receiver decisions on the transmitted symbols when either $\|\boldsymbol{\epsilon}\|$ or SNR increase. Figure 2 shows the accuracy of the theoretical values for $\mathrm{Var}[\hat{\epsilon}_{1,k}]$ with respect to the experimental ones.

To demonstrate the use of the proposed 2-D TED in a 2-D PLL, Figure 3 shows the symbol error probability $P_e \triangleq \frac{1}{N^2}\sum_{\mathbf{i}} \Pr[\hat{a}_{\mathbf{i}} \neq a_{\mathbf{i}}]$ for 4-PAM as a function of SNR with desynchronization offset $\boldsymbol{\tau}$. For comparison purposes, we also show the cases where the decoder uses $\hat{\boldsymbol{\tau}} = \mathbf{0}$ (no synchronization) and $\hat{\boldsymbol{\tau}} = \boldsymbol{\tau}$ (ideal synchronization). The 2-D PLL used updates its timing estimates according to the recursion $\hat{\boldsymbol{\tau}}_{k+1} = \hat{\boldsymbol{\tau}}_k - \mathrm{diag}(\boldsymbol{\alpha})\hat{\boldsymbol{\epsilon}}_k$, where $\boldsymbol{\alpha} = (\alpha_1, \alpha_2)^T \in \mathbb{R}^{+2}$ is the PLL gain vector, chosen to trade off tracking agility against estimate noise attenuation. The 2-D TED is operated in DD mode and the receiver assumes $\hat{\boldsymbol{\tau}}_1 = \mathbf{0}$. The increasing gap in P_e between the case where $\boldsymbol{\tau} = \mathbf{0}$ and the case where the PLL is used is due to the fact that as the SNR increases, the variance of the estimators becomes more important than the noise distortion.

c) Comparison with 1-D M&M TED: In order to demonstrate the advantages of our two-dimensional extension we compare it here to the adaptation of the one-dimensional M&M TED proposed in [1] to a two-dimensional setting. To this end, the timing functions (2) are estimated from the received signal using the 1-D M&M TED separately on the horizontal and vertical directions. This requires that the two estimators are built using different one-dimensional pasts. The estimators in this case take the form

$$\hat{\epsilon}^{\mathrm{1D}}_{1,k} = \left(z_{i-1,j}a_{i,j} - z_{i,j}a_{i-1,j}\right)/2\mathrm{E}[a^2]\ , \quad \hat{\epsilon}^{\mathrm{1D}}_{2,k} = \left(z_{i,j-1}a_{i,j} - z_{i,j}a_{i,j-1}\right)/2\mathrm{E}[a^2], \tag{19}$$

with $\hat{\epsilon}^{\mathrm{1D}}_{1,k}$ built using the past $\mathbf{z}_k^T = (z_{i-1,j}, z_{i,j})$ and $\hat{\epsilon}^{\mathrm{1D}}_{2,k}$ built using the past $\mathbf{z}_k^T = (z_{i,j-1}, z_{i,j})$, i.e., the estimators are built using a one-dimensional past along each dimension. We compare next the statistics of the 1-D estimators in (19) to those of the proposed 2-D estimators in (16) and (17). It is straightforward to show that $\mathrm{E}[\hat{\epsilon}_{l,k}] = \mathrm{E}[\hat{\epsilon}^{\mathrm{1D}}_{l,k}] = f_l(\boldsymbol{\epsilon})$ for $l = 1, 2$. Figure 4 shows the variance difference $\mathrm{Var}[\hat{\epsilon}^{\mathrm{1D}}_{1,k}] - \mathrm{Var}[\hat{\epsilon}_{1,k}]$ (similar results are obtained for $\hat{\epsilon}_{2,k}$). Notice that the reduction in variance achieved by the 2-D TED over the 1-D TED increases as the timing error moves further away from $\boldsymbol{\epsilon} = \mathbf{0}$. This owes to the fact that the 1-D estimator treats contributions from symbols in the other dimension as noise, and the magnitude of these contributions is greater for larger values of $\boldsymbol{\epsilon}$. By posing the problem in two dimensions, the derived 2-D TED does use this information in the estimation and hence the observed variance reduction. Notice also, that this variance reduction may be further lowered by exploiting all elements of $\mathcal{P}_k^{(2)}$.

V. Conclusions

We have presented a two-dimensional extension of the Mueller & Müller TED originally developed for one-dimensional channels. The advantage of using this 2-D TED over two separate 1-D TEDs operating in each dimension has been demonstrated. We have also built a 2-D PLL with this TED and demonstrated its ability to perform two-dimensional timing recovery. As aforementioned, recent applications such as multi-level 2-D bar codes and image data-hiding, may benefit from this 2-D PLL.

References

[1] K. H. Mueller and M. Müller, "Timing recovery in digital synchronous data receivers," *IEEE Transactions on Communications*, vol. 24, pp. 516–531, May 1976.

[2] J. R. Barry, A. Kavčić, S. W. McLaughlin, A. Nayak, and W. Zeng, “Iterative timing recovery,” *IEEE Signal Processing Mag.*, Jan 2004.

[3] N. Degara-Quintela and F. Pérez-González, “Visible encryption: Using paper as a secure channel,” in *Procs. of SPIE: Security and Watermarking of Multimedia Contents V*, vol. 5020, Santa Clara, USA, Jan 2003, pp. 413–422.

[4] R. Villán, S. Voloshynovskiy, O. Koval, and T. Pun, “Multilevel 2D bar codes: Towards high capacity storage modules for multimedia security and management,” in *Procs. of SPIE: Security, Steganography, and Watermarking of Multimedia Contents VII*, vol. 5681, San Jose, USA, January 16–20 2005, pp. 453–464.

[5] K. Whelan, F. Balado, G. Silvestre, and N. Hurley, “PLL-based synchronization of dither-modulation data hiding,” in *In Procs. of International Conference on Acoustics, Speech and Signal Processing, ICASSP*, Toulouse, France, May 2006.

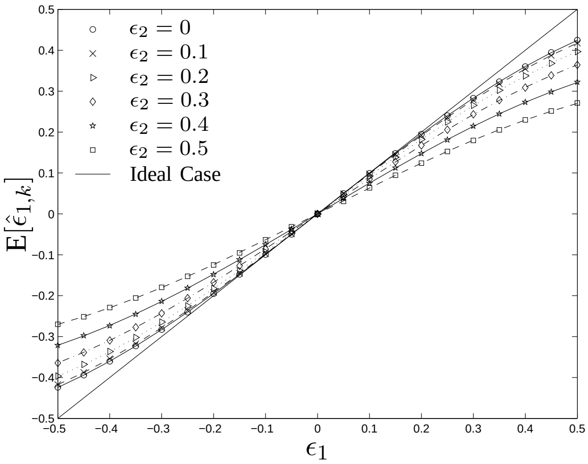

Fig. 1. $\mathrm{E}[\hat{\epsilon}_{1,k}]$ for 4-PAM with $h(\mathbf{t}) = \bar{h}(t_1) \cdot \bar{h}(t_2)$ and $\bar{h}(t) = \mathrm{sinc}(t/T)$. SNR $= 25$ dB. Markers indicate experimentally measured $\mathrm{E}[\hat{\epsilon}_{1,k}]$ with corresponding lines representing $f_1(\boldsymbol{\epsilon})$ for different values of ϵ_2.

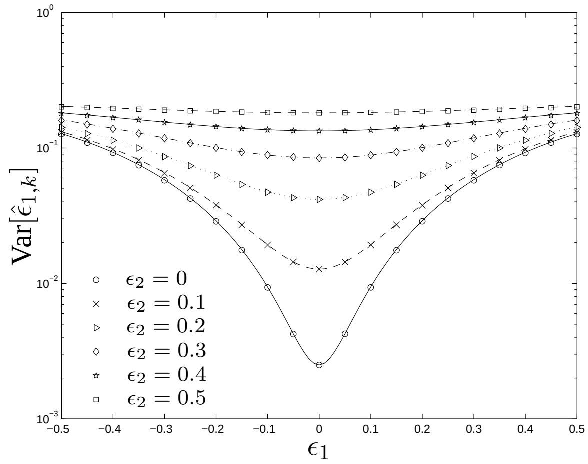

Fig. 2. $\mathrm{Var}[\hat{\epsilon}_{1,k}]$ for 4-PAM with $h(\mathbf{t}) = \bar{h}(t_1) \cdot \bar{h}(t_2)$ and $\bar{h}(t) = \mathrm{sinc}(t/T)$. SNR $= 25$ dB. Markers indicate experimental values while corresponding lines represent theoretical values computed from (18).

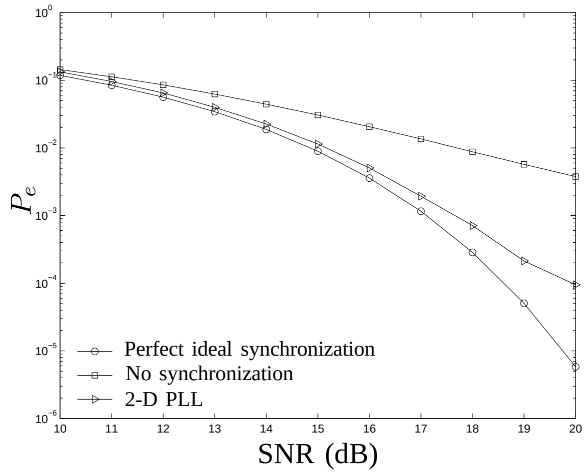

Fig. 3. Symbol error reduction achieved using 2-D PLL on 4-PAM with $h(\mathbf{t}) = \bar{h}(t_1) \cdot \bar{h}(t_2)$ and $\bar{h}(t) = \mathrm{sinc}(t/T)$. $\boldsymbol{\alpha} = 0.02 \cdot \mathbf{1}$, $\boldsymbol{\tau} = 0.05 \cdot \mathbf{1}$.

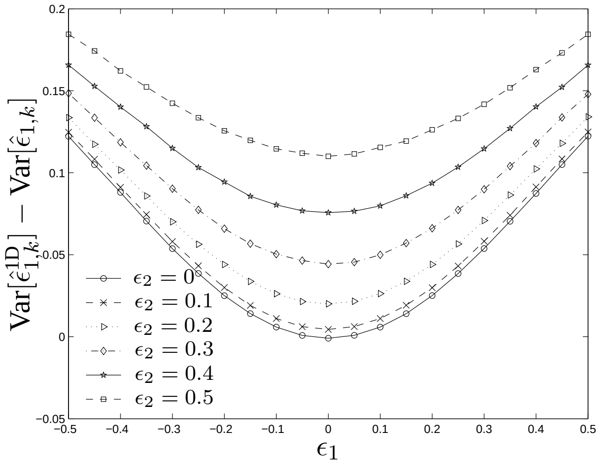

Fig. 4. Variance reduction $\mathrm{Var}[\hat{\epsilon}_{1,k}^{\mathrm{1D}}] - \mathrm{Var}[\hat{\epsilon}_{1,k}]$ offered by using 2-D TED over two separate 1-D TEDs for 4-PAM with $h(\mathbf{t}) = \bar{h}(t_1) \cdot \bar{h}(t_2)$, $\bar{h}(t) = \mathrm{sinc}(t/T)$ and $\mathrm{E}[\hat{\epsilon}_{1,k}] = \mathrm{E}[\hat{\epsilon}_{1,k}^{\mathrm{1D}}] = (h_{-1,0} - h_{1,0})/2$. SNR $= 25$ dB.